Geogr. Fis. Dinam. Quat.
35 (2012), 141-152, 9 figg., 1 tab.

DOI 10.4461/GFDQ.2012.35.13

ELEONORA REGATTIERI (*), ILARIA ISOLA (**), GIOVANNI ZANCHETTA (*,**,*****), RUSSEL N. DRYSDALE (***), JOHN C. HELLSTROM (****) & ILARIA BANESCHI (*****)

STRATIGRAPHY, PETROGRAPHY AND CHRONOLOGY OF SPELEOTHEM DEPOSITION AT TANA CHE URLA (LUCCA, ITALY): PALEOCLIMATIC IMPLICATIONS

ABSTRACT: REGATTIERI E., ISOLA I., ZANCHETTA G, DRYSDALE R.N., HELLSTROM J.C. & BANESCHI I., *Stratigraphy, petrography and chronology of speleothem deposition at Tana che Urla (Lucca, Italy): paleoclimatic implications* (IT ISSN 0391-9838, 2012).

In this work we present the results of a stratigraphic and lithologic study of a flowstone from Tana che Urla Cave, Apuan Alps (central Italy) which grew intermittently between ca. 160 and 8 ka. The studied succession consists of an alternation of two different lithofacies (Lf-A, Lf-B): a brown, detrital-rich (Lf-A) and a white, inclusion-poor calcite (Lf-B). Using available growth rate data, the difference between the two lithofacies is thought to be the result of different amounts of meteoric precipitation, with Lf-A related to low growth rates at times of low precipitation during phases of climatic deterioration (stadial or glacial) and a higher flux of clastic material, and Lf-B related to high growth rates due to high infiltration under conditions of higher precipitation during wetter (interstadial/interglacial) periods, with lower clastic flux. Following this interpretation and the available chronology, the flowstone investigated shows a basal portion of Lf-A that was deposited during MIS6. The flowstone then passed from Lf-A to Lf B at the MIS6-5 transition, with Lf-B lasting for the full interglacial of MIS5e. A long growth interruption (hiatus H1) can be correlated with the MIS5d stadial, with resumption of lithofacies Lf-B occurring during the climatic amelioration of interstadial MIS5c. The age profile of the upper part of the flowstone is poorly constrained, and is characterised by several growth interruptions, suggesting that the last glacial was more severe compared to MIS6.

KEY WORDS: Speleothems, Tana che Urla, Central Italy; Lithofacies, MIS5.

RIASSUNTO: REGATTIERI E., ISOLA I., ZANCHETTA G, DRYSDALE R.N., HELLSTROM J.C. & BANESCHI I., *Stratigrafia, petrografia e cronologia di speleotemi della Tana che Urla (Lucca): implicazioni paleoclimatiche*. (IT ISSN 0391-9838, 2012).

In questo lavoro vengono presentati i risultati dello studio stratigrafico e litologico di un flowstone della grotta Tana che Urla, Alpi Apuane (Italia centrale), cresciuto in modo intermittente tra circa 160 e 8 ka. La successione studiata consiste nell'alternanza di due diverse litofacies: una marrone, ricca in detrito (Lf-A) e una bianca, composta di calcite pura (Lf-B). Basandosi sui dati disponibili sul tasso di crescita, la differenza tra le due litofacies viene considerata come il risultato di differenti quantità di precipitazioni meteoriche, con Lf-A legata a bassi tassi di crescita dovuti a scarse precipitazioni durante fasi di deterioramento climatico (glaciali/stadiali) e Lf-B legata ad alti tassi di crescita dovuti a una maggiore infiltrazione in relazione a maggiori precipitazioni durante periodi più umidi (interglaciali e interstadiali). Seguendo questa interpretazione e la cronologia disponibile, il flowstone oggetto dello studio mostra una parte basale di Lf-A deposta durante il MIS6, il passaggio tra Lf-A e Lf-B alla transizione MIS6-5 e la presenza di Lf-B durante le condizioni pienamente interstadiali del MIS 5e. La principale interruzione della crescita (Hiatus H1) può essere correlata con lo stadiale MIS 5d e il riapparire della Lf-B con il miglioramento climatico legato all'interstadiale MIS 5c. La parte superiore del flowstone ha una cronologia poco definita ed è caratterizzato da una serie di interruzioni della crescita che suggeriscono come l'ultimo glaicale (MIS 4-2) sia stato caratterizzato da condizioni più severe rispetto al MIS 6.

TERMINI CHIAVE: Speleotemi; Tana che Urla; Italia centrale; Litofacies; MIS5.

INTRODUCTION

Speleothems are secondary carbonates formed in caves from percolation waters rich in $CaCO_3$ by the precipitation of calcite (or aragonite) due to the principal mechanism of CO_2-outgassing (Ford & Williams, 1989). Generally, they develop in climatic regions characterized by above freezing mean temperatures, with enough rainfall and soil biological activity to promote solute transport into the cave environment (Gascoyne, 1992).

(*) *Dipartimento di Scienze della Terra, University of Pisa, Via S. Maria, 53 - 56126 Pisa, Italy.*
(**) *Istituto Nazionale di Geofisica e Vulcanologia, sezione di Pisa, Via della Faggiola 32 - 56100 Pisa, Italy.*
(***) *Department of Resource Management and Geography, University of Melbourne - Victoria 3010, Australia.*
(****) *School of Earth Sciences, University of Melbourne - Victoria 3010, Australia.*
(*****) *IGG-CNR Via Moruzzi, 1 - 56100 Pisa, Italy.*
Presented at FIST - VIII Forum Italiano di Scienze della Terra, Torino, 19-23 September 2011.
We thanks L. Dallai and M. Guidi for the facility support at IGG-CNR of Pisa. We thank Sophie Verheyden and another anonymous reviewer for the suggestions and the criticisms which improved the quality of the manuscript and its readability.

The composition of drip water depends largely on the outside climate conditions such as temperature, amount of rainfall, precipitation sources and on the soil biological activity (which is itself climate-driven too). Changes in these parameters produce a variable signal in the chemistry of the cave waters which is transferred in many speleothem via properties such as the isotopic composition of oxygen and carbon in the calcite, the composition of trace elements and the growth rate (Lauritzen & Lundberg, 1999), producing archives capable of yielding multi-proxy palaeoenvironmental records that cover, potentially and often continuously, many millennia. Moreover, speleothems possess the great advantage of being precisely and accurately datable using U-series techniques (Li & *alii*, 1989*;* Hellstrom, 2003) and can thus be used to test theories of climate forcing and reveal the timing, magnitude, duration and geographic extent of global and regional climatic events (Wang & *alii*, 2001*;* Spotl & Mangini, 2002; Genty & *alii*, 2003; Spotl & *alii*, 2002; Drysdale & *alii*, 2009).

Although the most used of speleothem properties for reconstructing past climate (especially palaeo rainfall, e.g. Ayalon & *alii*, 2002) is the stable isotope composition of oxygen and carbon ($\delta^{18}O$ and $\delta^{13}C$), recent works (e.g. Zhornyak & *alii*, 2011, Meyer & *alii*, 2012) have focussed their attention on stratigraphy and detrital content of speleothems in order to obtain new insights into Earth-surface processes, that operated in the infiltration area during the time of speleothem formation, and into palaeohydrological processes (Niggemann & *alii*, 2003; Jaillet & *alii*, 2006), and to disentangle the climatic signal related to that processes.

Detrital components in cave sediments comprise particles and colloids that are produced by the weathering of bedrock and soil, and are subsequently transported into the karst system; this detrital phase can be incorporated in speleothems as macroscopically visible layers of mud or silt (Niggemann & *alii*, 2003; Jaillet & *alii*, 2006; Zhornyak & *alii*, 2011) or, more commonly, as microscopic particles concentrated in individual layers of calcite. Changes in quantity and type of clastic components may affect also a speleothem's fabric (Frisia & *alii*, 2000; 2003) and the composition of some trace elements commonly bound to detrital particles and/or colloids, e.g. Fe, Mn, Zn, Th, and Rare Earth Elements (e.g. Ayalon & *alii*, 1999; Fairchild & Treble, 2009).

In this study, we describe the stratigraphy, the petrography and the chronology of two cores from a flowstone in Tana che Urla Cave, in the Apuan Alps (Central Italy), which was deposited intermittently during the penultimate glacial (MIS6), the last interglacial (MIS5) and part of the last glacial (MIS 4-2). This succession includes several growth interruptions (hiati) and ends with the Holocene (MIS1). The two cores show different petrographic facies, with the alternation of detrital-rich and detrital-poor calcite, with both having very different growth rates. This suggests environmental changes during the flowstone growth and our purpose is to define depositional and palaeoenvironmental models in order to explain the formation of this characteristic calcite succession.

STUDY AREA, MATERIALS AND METHODS

The Tana che Urla (fig. 1) is a small spring-cave (592 m of total length, 370 m emerged and 222 m submerged; +45 m of total height difference) with a permanent streamway that flows from the interior to the entrance. This cave is one of the best known in the area and was first described in 1723 by the famous naturalist Antonio Vallisneri, in his book «*Lezione accademica sull'origine delle Fontane*» (Academic lesson on spring's origins).

The entrance is located at 620 m asl on the south-eastern side of the Apuan Alps, on the Panie massif, a small group of peaks which reach a maximum height of 1859 m (Pania della Croce), and which together comprise part of the Apuan Alps Metamorphic Core Complex (MCC) (Carmignani & Klingfield 1990). In the Turrite di Gallicano valley, where Tana che Urla is located, the contact between the MCC and the non-metamorphic unit outcrops (fig. 1). The cave developed at the contact between Triassic schist and the Triassic meta-dolomite knows as Grezzoni (fig. 2).

The subterranean stream flowing through the cave is probably the terminal part of an underground collector

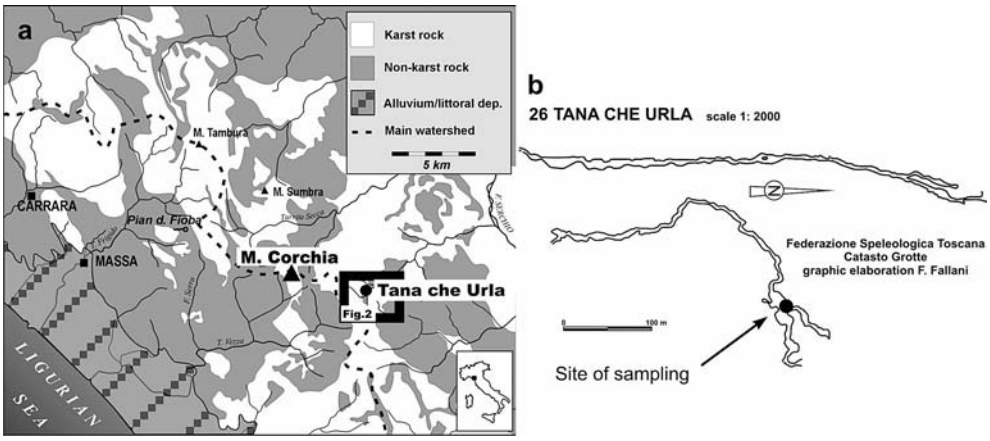

FIG. 1 - Site location (a) and map of the Tana che Urla cave (b).

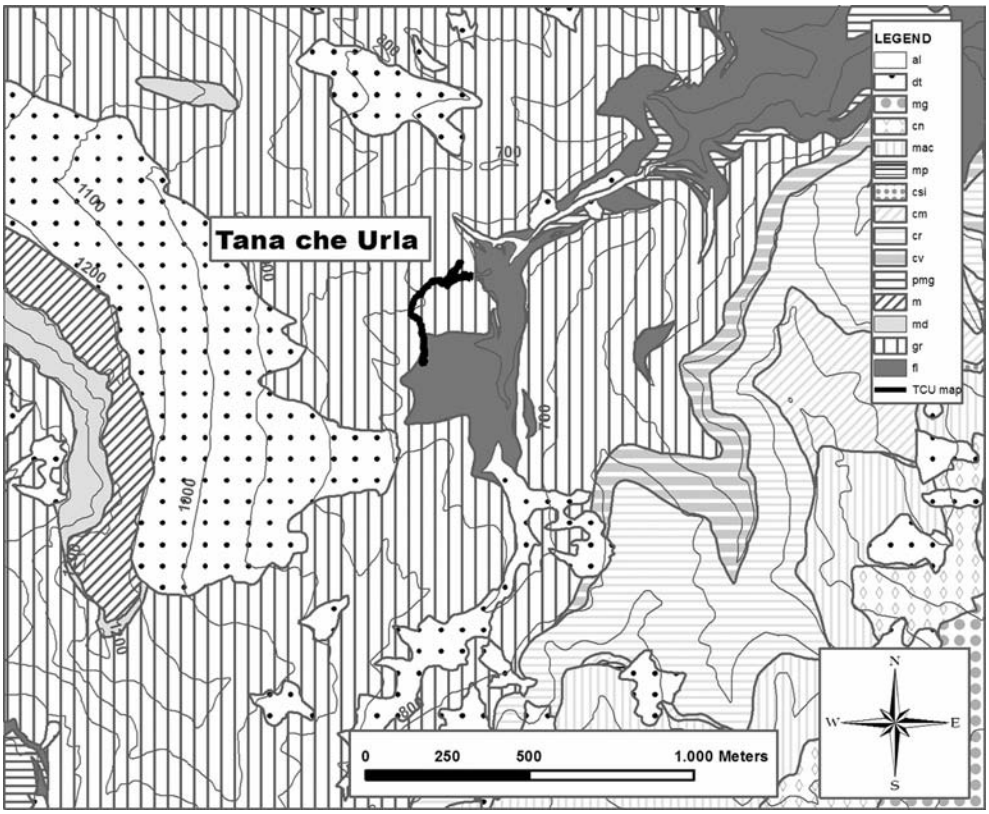

FIG. 2 - Geologic overview of the study area, with the the plan of TCU cave shown in black (modified from Carmignani & *alii*, 2000). Quaternary deposits: al = fluvial deposits dt = slope debris deposits. Non metamophic units: mg = macigno sandstone Early Oligocene-Late Miocene, cn = calcari a nummuliti Eocene-Late Oligocene, mac = maiolica Ealry Titoniano-Late Cretceo, mp = marne a posidonia Late Toarciano-Calloviano, csi = Calcari selciferi a entrochi Medium-Upper Lias, cm = calcare massiccio Hettangiano, cr = calcari e marne a Rhaetavicula contorta Norico-Retico, cv = calcare cavernoso, brecce poligeniche Norico-Retico. Metamorphic Units: pmg = metasandstone Upper Oigocene, m = marble Late Lias, md = dolomitic marble Retico, gr = dolostones Norico. Paleozoic Basement: fl = Filladi inferiori Cambriano-Ordoviciano.

that drains the southern slope of Pania della Croce, which therefore represents the catchment area of the cave.

The valley above the cave is covered by a relatively deep soil and sustains a forest comprised mainly of chestnut (at lower altitude) and beech (at higher altitude), while the summit part of the slope hosts a grassland of *Brachipodium* ssp.

The climate in this area is wet throughout the year, with abundant rainfall during fall and spring, many days of snow during winter and intense rain storms during summer. The mean annual precipitation is about 2500 mm in the nearby village *of Fornovolasco* (data recovered from 1951 to 1995, Piccini & *alii*, 1999) but probably higher (more than 3000 mm/years) on the ridge of the Pania. There is no outside air temperature record but the mean annual temperature (MAT) of the cave is 10.2 °C.

Tana che Urla is close to the more famous Corchia Cave, so it is possible to find an exhaustive geological, geomorphological and climatic setting of the area from previous studies of Corchia, especially on Piccini (1997, 2008, 2011), Piccini & *alii* (2003) and in Drysdale & *alii* (2004).

In 2007 several cores were drilled within the cave using a 38 mm-OD/34 mm-ID diamond-cut corer connected to an electric drill (Milwaukee Electric tools, with 28 volts of power and lithium-ion batteries). Two of these cores, TCUD3 and TCUD4 (herein called D3 and D4), collected from the same flowstone are the subject of this note. D4 and D3 are 350 mm and 640 mm long, respectively. In both cores the bedrock was reached. The two cores show several different lithological features (discussed in detail below) and some evidence of growth interruptions, in some cases with evidences of erosion and mud deposition.

D3 and D4 were investigated macroscopically and using thin sections for characterising different lithofacies. The thin sections were analyzed with a transmitted light microscope (Leica DMRX) and photographed with a digital camera (Leica DFC 320). Description of the thin sections followed Frisia & *alii* (2000, 2003).

Polished sections of the two cores were sub-sampled for stable isotopes. D4 was sampled at 1 mm increments using a milling machine (CNC Micro Proto System) with a 1 mm-diameter drilling bit, producing 350 subsamples. D3 was sampled with a manual drill (1 mm-diameter drilling bit) at ca. 1.5-2,0 mm of increments, producing 393 subsamples. Stable oxygen ($\delta^{18}O$) and carbon ($\delta^{13}C$) isotope ratios analysis were performed using a GV Instruments GV2003 continuous-flow Isotope-Ratio Mass Spectrometer (IRMS) at the Newcastle University (NSW, Australia). Sample results were normalised to the V-PDB scale using a Carrara Marble standard (NEW1) previously calibrated using the international standards NBS-18 and NBS-19. Analytical uncertainty for $\delta^{18}O$ and $\delta^{13}C$ were 0.09‰ and 0.05‰ respectively.

Sub-samples were also taken from both cores for U/Th dating, initially as powder (manually with a traverse of 1 mm-diameter holes along a single growth lamina) but, because of the large uncertainty of the initial results owing to high detrital contamination and low uranium content, subsequently small prisms of ca. 300 mg were taken.

The U/Th dating was performed on a Nu-Instruments Plasma Multi-Collector Inductively Coupled Plasma-Mass Spectrometer (MC-ICPMS) using the method of Hellstrom (2003) at the University of Melbourne (Victoria, Australia). Briefly, samples were dissolved and a mixed ^{236}U-^{233}U-^{229}Th spike was added prior to removal of the carbonate matrix with ion-exchange resin. The purified U and Th fraction was introduced in a dilute nitric acid to the MC-ICP-MS. The $^{230}Th/^{238}U$ and $^{234}U/^{238}U$ activity ratios were calculated from the measured atomic ratios using an internally standardised parallel ion-counter procedure and calibrated against the secular equilibrium standard, HU-1. Corrections for the detrital Th content were applied following Hellstrom (2006).

RESULTS

Lithography and stratigraphy

Both cores are mainly composed of columnar calcite, from poorly laminated to massive, often with a consistent detrital component. Based on the clastic content, the calcite fabric and the macroscopic aspect and colour of the calcite, several lithofacies (Lf) were defined. These facies are slightly different for the two cores but allowed us to make a convincing correlation between them. Lithofacies and stratigraphic correlation of the flowstone are schematized in fig. 3. To facilitate the following discussion, every section is labelled with a number, independent from the corresponding lithofacies. The TOP section in the same figure indicates the terminal part of the flowstone which, due to the large number of growth interruptions, did not allow us to define a precise lithofacies.

The flowstone sequence is most complete in D3, so we choose it as the master core. The succession starts with Lithofacies A. This lithofacies is the most rich in clastic material and it is characterised by grey-brown calcite with thin laminations of detritus. This lithofacies can be divided in two sub lithofacies (S-Lf A1 and A2) with a decrease in the detrital content in A2.

A1 is only found at the bottom part of D3 (section 1, from 640 to 510 mm from the top) and represents the darker part of the flowstone, with thinner laminations of clastic components. It begins with a columnar-like fabric with small crystals (fig. 4a-1). In some positions, the growth of the single crystals is quite disturbed: the boundaries are irregular and some microstructures like dislocations and sub-grains are present. Immediately above, the structure changes and the calcite becomes columnar, with bigger and well-developed single crystals, but not fully coalescent. The space between the crystals is filled by laminated detritus, with an alternation between dark material (possibly oxides, clay and/or organic material) and light calcareous sand (fig. 4a-2).

The sub-lithofacies A2 (fig. 4c-1) is lighter and browner in colour than A1 and the thickness of clastic laminae is greater than in A1. A2 is present in different positions of both cores (three times in D3: section 2, from 510 to 420, section 4, from 310 to 280 and section 6, from 245 to 210 mm from the top; twice in D4: section 8, from the bottom, 350, to 210 and section 10, from 120 to 80 mm from the top). The fabric is columnar, with regular, coalescent crystals. The detrital content forms laminations which cross the crystals without disturbing their growth. The second layer of A2 in both cores (section 4 in D3 and section 10 in D4) is crossed by a big growth interruption (hiatus H1).

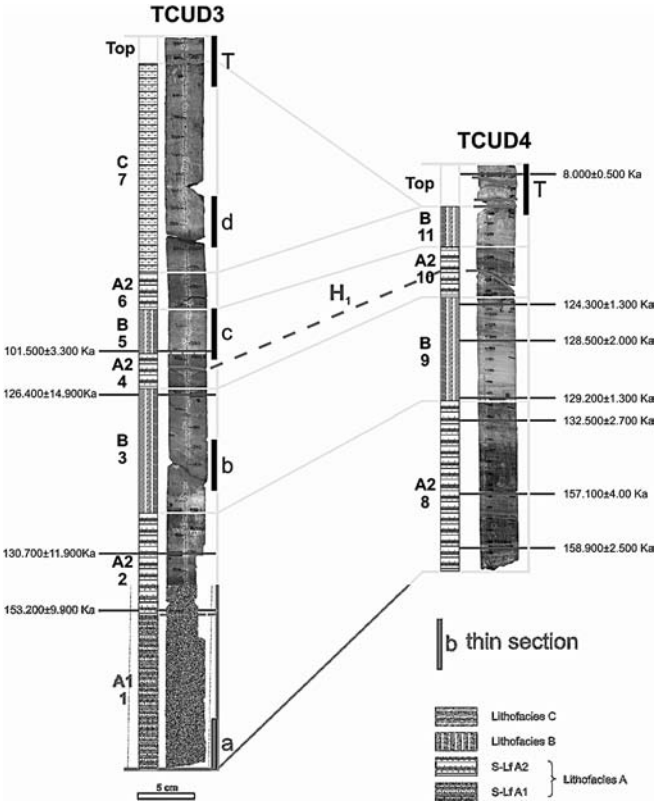

FIG. 3 - Petrography and U/Th ages of the TCU cores and the proposed stratigraphic correlation between the cores. Progressive numbers indicate the different sections described in the text.

The central part of both cores is included within the lithofacies B2. It is made of compact, milky calcite, with no evidence of laminations and few impurities. In D3 this interval extends over a greater core depth than in D4. In the succession we found Lf-B twice in both cores (in alternation with A2), in D3 from 420 to 310 (section 3) and from 280 to 245 mm from the top (section 5) and in D4 from 210 to 120 (section 9) and 80 to 40 mm (section 11) from the top. The fabric is mostly columnar (fig. 4b and 4c-2) with large, regular crystals with straight boundaries and no evidence of clastic deposition.

The last defined lithofacies, Lf-C (fig. 4d), is present only in D3, from 210 to 50 mm from the top (section 7). In this section the calcite is yellowish and more porous than Lf-B with little detrital content and no laminations. Lf-C shows structures that suggest the presence of micro-pools on the flowstone surface, with small holes filled by pseudo-geopetal structures of calcite (well developed crystals)

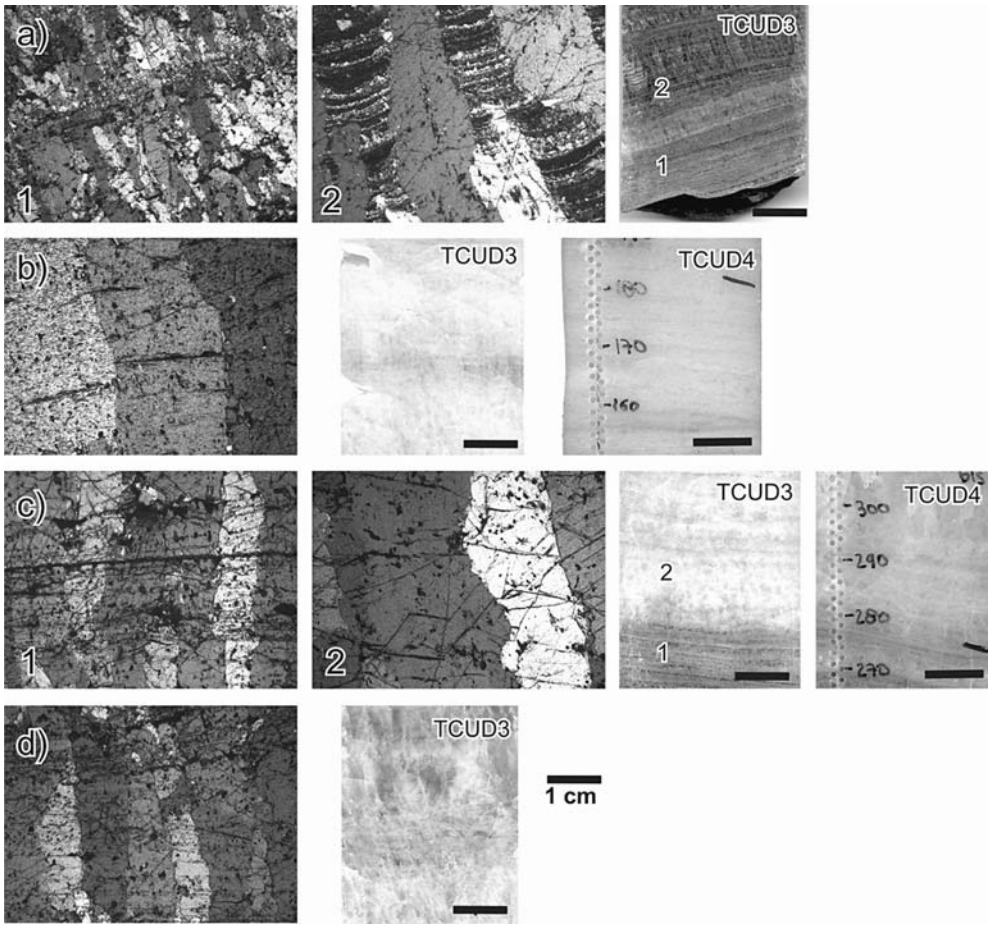

FIG. 4 - a) Thin section from sublithofacies A1 in TCUD3: 1 - columnar calcite fabric with small, disturbed, crystals at the very bottom of the core. 2 - still shows a columnar fabric but with larger crystals, non-coalescent and with laminated detritus (base of microphotograph: 5,74 mm). In the photo on the right, the bottom of core TCUD3, depth 640-610 mm from the top. b) Thin section from TCUD3 and photos from Lithofacies B. Note the milky colour of the calcite and the mostly columnar fabric, with large crystals, straight boundaries and few impurities. c) (1) Sub lithofacies A2 in D3. Note the columnar fabric with detrital laminations. (2) Lf B in TCUD3. In photos, on the left the transition from A2 and B in D3 (from 270 to 240 mm from the top), on the right the same transition in D4 (from 100 to 50 mm from the top). d) Sublithofacies C in D3. Note the intermediate texture between S-Lf A2 (for the crystal size) and Lf B (for the detrital content). Photo on the right from 120 to 90 mm from the core top). All microphotographs of the thin sections were taken under crossed nicols.

(fig. 5). The fabric is still strongly columnar with few impurities, as in Lf-B, but the size of the crystals is smaller, and more similar to S-Lf-A2. The absence of this lithofacies in the other core may be related to the relative position of the cores on the flowstone: it is probable that during the deposition of this phase the point of D3 was subtabular (in fact we have micro-pool structures, related to a slight slope and slow water flow) while the point of D4 (which is in a lower lobe of the flowstone) was probably to steep to allow the deposition and/or the lobe was out of the depositional path.

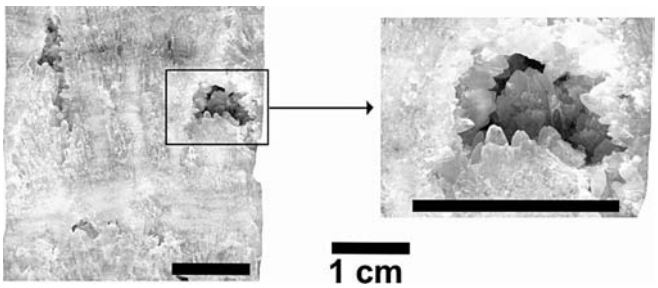

FIG. 5 - Details of Lf-C (core D3) showing small cavities with calcite pseudo-geopetal structures, probably related to microgours on the flow stone's surface.

The top part of both cores reveals an interesting series of growth interruptions (fig. 6). Although this part does not have a defined chronology, we can classify these discontinuities as real *hiati* because in thin section they clearly show erosive surfaces and mud deposition and, moreover, evidences of non-continuity in the calcite deposition and fabric.

Looking in detail, in D3 we can detect at least 4 interruptions (shown by black arrows in fig. 6). The first (arrow α) separates section 7 (columnar, Lf-C) from a little layer of microcrystalline calcite which is followed by a complex structure (arrow β), which includes several layers of clastic deposition (which brings growth cessation and maybe further erosion) embedded with several phases of re-growth, still with a microcrystalline structure. Following this is a 1 cm thick layer of yellow, columnar calcite, which stops again at another hiatus (arrow γ) then over the last two centimetres we observe white, columnar calcite, crossed by the last hiatus (arrow δ). In D4 the fabric looks very similar, with at least three main interruptions, the second of which (arrow ζ) is probably the same as the second one in D3 (arrow β).

Isotopic data

A detailed discussion of the isotopic record is outside the aim of this paper but the correlation between $\delta^{13}C$ and

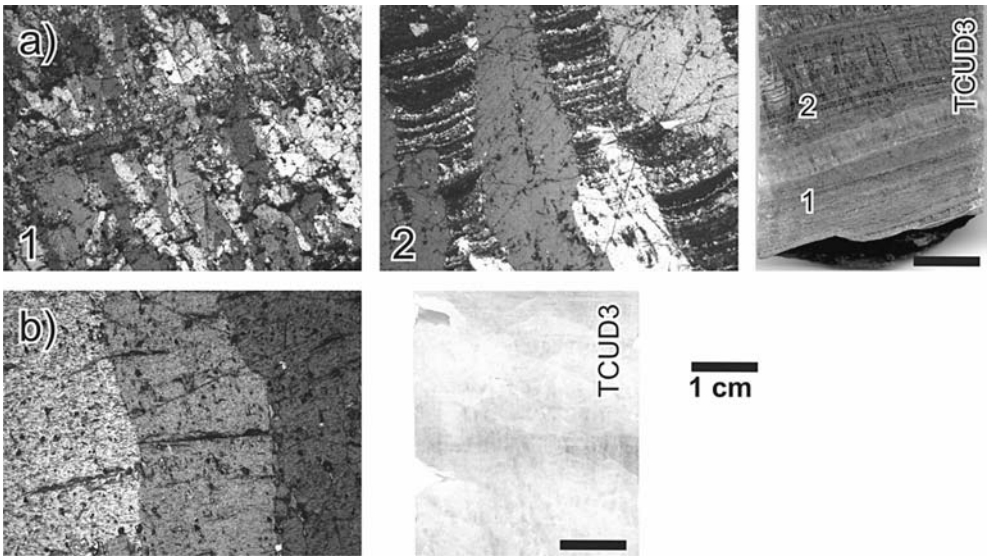

FIG. 6 - The top part of the two cores, hiati marked by small Greek letters. Base of microphotographs 5,74 mm, taken under crossed nicols.

$\delta^{18}O$ (fig. 7) suggests that there is a connection between isotopic composition and petrography in these flowstone samples, although every lithofacies partly overlaps in its $\delta^{13}C$ and $\delta^{18}O$ values. Lithofacies A has the highest isotopic values whereas Lf-B presents slightly lower $\delta^{18}O$ and $\delta^{13}C$ values. Furthermore, in Lf-A there is large variation in both the $\delta^{13}C$ (ca. 10‰) and the $\delta^{18}O$ (ca. 4‰) while Lf-B shows less variability and a variation in the $\delta^{13}C$ (ca. 6‰) which contrasts with the rather small changes in $\delta^{18}O$ (ca. 2‰). Lf-C exhibits intermediate values and the smallest range of variations: ca. 2‰ for $\delta^{18}O$ and 4‰ for $\delta^{13}C$.

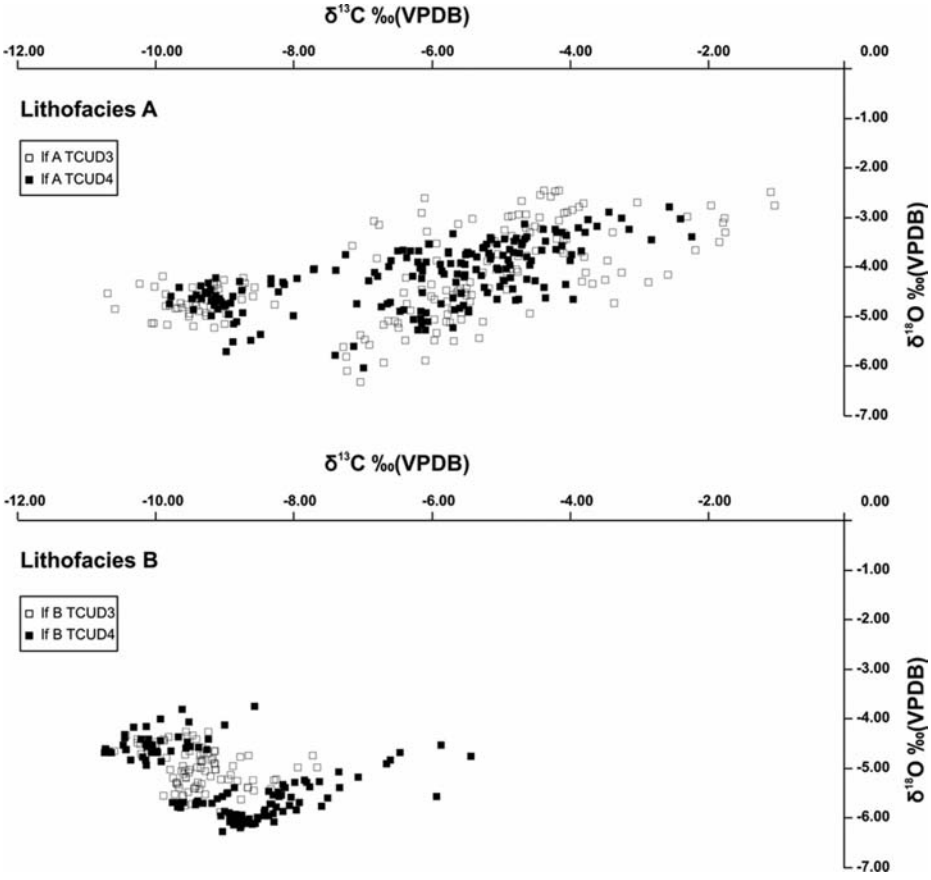

FIG. 7 - Correlation between $\delta^{18}O$ and $\delta^{13}C$ of the same lithofacies (A and B) in both cores. Full squares represent core TCUD4, and empty squares represent core TCUD3.

The proposed correlation between the cores is also strengthened by the analysis of the isotopic composition (fig. 8). Indeed, the $\delta^{13}C$ and $\delta^{18}O$ values of the same lithofacies in both cores are tightly linked.

Chronology and growth rates

The high detrital Th component linked to the clastic contamination within the cave brings a large uncertainty for some of the measured ages. To build our chronology, we select just the ages affected by the least contamination (table 1) (i.e. with lower error and high correlation between uncorrected and corrected ages); the more unreliable ages have been discarded because they yielded unacceptably large age uncertainties. In particular, for TCUD3 A_d and TCUD3 Abis C, it is difficult to correct the original clastic contamination due to the lack of at least one good age in the overlying part of D3, which could be used as an upper limit for the correction.

It is interesting to note that the quantity of detrital Th is different in the different lithofacies, with cleaner samples and better ages obtained from the white calcite of Lf-B, and larger errors related to Lf-A. Age measurement, U and Th content and corresponding lithofacies are reported in table 1.

According to the U/Th ages, the flowstone spans from ca.160 ka to 8 ka, although deposition was not continuous and the growth probably stopped for long periods. Considering the age and the position of the mayor growth interruption (H1), it is possible to identify a period of continuous growth between ca. 158,9 ± 2.5 ka and ca. 124,3 ± 1,3 ka. This period includes sections 1, 2 and 3 in D3 and sections 8 and 9 in D4, and is followed by the mayor growth interruption (hiatus H1). Above H1 only two more ages are available: one in D3 just after H1 (ca. 101.5 ± 3.3 ka) which indicates that H1 corresponds to an interruption of deposition between ca. 124 and ca.101 ka. After H1 there are no evidence of growth interruption until the terminal section, but for this part we have insufficient dating to constrain the chronology of the upper part of the flowstone. The last available age is at the very top of D4, after the terminal series of *hiati*, and it is Holocene in age (8,05 ± 0.49 ka).

Looking in detail at the age of the different sections of the defined lithofacies, we can broadly fix the first part of Lf-A (sections 1, 2 and 8) between 160 and 130 ka while the age of the first layer of Lf-B (sections 3 and 9) is almost certainly within the interval 130 and 124 ka. Hiatus H1 separates section 3 and 9 from the second part of Lf-A

TABLE 1 - U/Th ages for TCUD4 and TCUD3; marked with an asterisk are the ages rejected due to the large uncertainness and the low (under 90%) correlation between uncorrected and corrected values

Core	Sample ID	Depth	$^{230}Th/^{238}U$	$^{234}U/^{238}U$	Uncorrected Age (Ky)	Corrected Age (Ky)	2se	Age Cr/Age	Lf
TCUD4	TCUD4-D	8.5	0.1023	1.3521	8.5	8.0	0.5	95%	T
	TCUD4-C	123.5	0.8130	1.1631	125.2	124.3	1.3	99%	B
	TCUD4-4	156.5	0.8746	1.2233	128.8	128.6	2.1	100%	B
	TCUD4-B	207.5	0.8845	1.2295	130.1	129.2	1.3	99%	B
	TCUD4-3	225.5	0.9073	1.2394	134.1	132.5	2.7	99%	A
	TCUD4-2	287.5	0.9509	1.1974	159.4	157.1	4.0	99%	A
	TCUD4-A	334.5	0.9361	1.1804	158.8	158.9	2.5	100%	A
TCUD3	*TCU D3 A_d	28.5	0.6701	1.2805	77.9	43.4	41.3	56%	C
	*TCU D3 Abis C	193.0	1.0634	1.2557	180.9	145.6	41.4	80%	C
	TCU D3 Abis.b	285.0	0.7642	1.2196	102.9	101.5	3.3	99%	B
	TCUD3 E	314.5	0.8858	1.1877	140.6	126.4	14.9	90%	B
	TCUD3 C	458.5	0.9059	1.2061	141.9	130.7	11.9	92%	B
	TCU.D3 B_e	509.5	0.9759	1.2165	162.0	153.2	9.9	94%	A

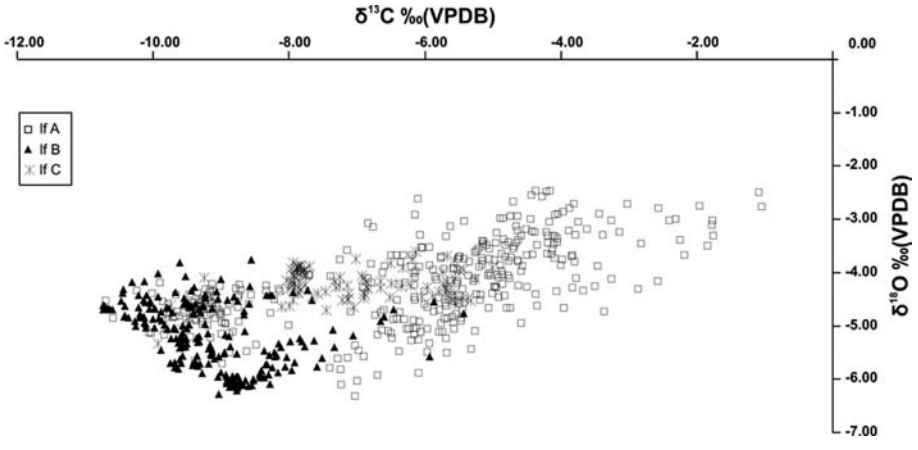

FIG. 8 - Correlation between $\delta^{18}O$ and $\delta^{13}C$ of the different Lithofacies (both cores together). Lf-A (empty squares) is characterized by the highest isotopic values and largest range of variation, both for oxygen (ca. 4‰) and carbon (ca. 9‰). Lf.B (full triangle) presents lower values and less variation, especially for $\delta^{18}O$ (ca. 2‰ for oxygen and 6‰ for carbon). Lf C (asterisk) shows intermediate values and variation range.

(sections 4 and 10), for which the only age available is ca. 101 ka. For the upper section, as noted previously, there are not enough data to constrain the chronology.

Regarding the growth rates, the available ages allow us to draw a very crude distinction between the first part of the cores (lf-A, sections 1,2 and 8) and the middle part (Lf-B, sections 3 and 9). Looking at D4, which is the best dated interval, we see that the growth rates change drastically at the passage between the two lithofacies: the first 140 mm from the bottom actually covers about 130 kyr, whereas the next 90 mm span ca. 5 kyr. This corresponds to a change in the growth rate from ca. 1,07 mm/kyr to 18 mm/kyr. Although these are only first-order calculations, they suggest that a large change happened in the cave environment between these two periods.

DISCUSSION

The calcite fabric in speleothems (defined as the organization of crystals within layers characterized by synchronous crystallization, Frisia & *alii*, 2000) is the result of the interplay of many factors, which have mostly an environmental control: the chemistry of drip waters (i.e. supersaturation and composition of trace elements), the drip rate and the rate of outgassing (Dreybrodt, 1988; Gonzalez & *alii*, 1992, Frisia & *alii*, 2000, Frisia, 2003).

A columnar calcite fabric (such as observed throughout the TCU cores) is demonstrated to form from fluids at low levels of supersaturation and where the speleothem surface is continuously wet (Gonzalez & *alii*, 1992; Frisia & *alii*, 2000, Frisia 2003). Macroscopic petrographic features also suggest that the TCU flowstone was covered by a continuous water film during its growth, because more or less the same lithofacies can be traced between the two cores. However, there are some differences in the thickness of individual calcite layers and an absence of Lf-C in D4: this indicates that flowstone growth rates were spatially and temporally variable.

The preliminary data on growth rate of TCU flowstone suggest a relationship between the growth rate and the petrography: if the flux of detrital material from the infiltration area was almost constant over time but rates of calcite deposition changed rapidly in response to climatic changes, one would expect white, detrital-poor calcite during periods of high infiltration and brown, detrital-rich calcite during drier periods. On the other hand, if the detrital flux was not constant (a more realistic situation) we would expect to have a higher detrital flux during glacial/stadial periods, with cold/dry conditions implying less well-developed soil and lower vegetation cover resulting in more detrital material transported via seepage water. During climatic amelioration instead, the higher discharge and the well developed soils and vegetation cover would produce the purest, white calcite with higher growth rates. Moreover, during cooler periods, the PCO_2 of the percolation water would be reduced because of lower plant CO_2 production in the soil, so this would reduce growth rate as well because the dissolved Ca would be lower.

For the western Mediterranean region, it is known that present-day temperature and rainfall amount are strongly controlled by North Atlantic circulation patterns (Bolle, 2003; Trigo & *alii*, 2002) and evidence for persistence of this influence through glacial periods is well-documented in marine-sediment (Chaco & *alii*, 1999) as well in continental records. In particular, for the Apuan Alps it has been demonstrated that variations in speleothems $\delta^{18}O$ are mainly governed by rainfall amount (Drysdale & *alii*, 2004; 2007; 2009; Zanchetta & *alii*, 2005, 2007) and largely reflect the variations in temperature of the North Atlantic Ocean, with higher evaporation and moisture advection in warmer periods (i.e. interglacials and interstadials), leading to an increase in precipitation, especially where the rainfall is mainly orographic, such as in the Apuan region.

Therefore, it is feasible that the brown, detrital-rich calcite sequence (Lf A) formed under conditions of lower percolation rates during periods of climatic deterioration (dry and cold climate) whilst the white, inclusion-poor calcite sequence (Lf B) coincident with warmer and wetter periods. The observed pattern of $\delta^{18}O$ and $\delta^{13}C$ values strengthens this environmental interpretation: the highest isotopic values are related to the brown facies whilst the lower values are associated with white calcite (Bard & *alii*, 2002) (fig. 7).

The available chronology for the TCU flowstone allowed us to define the period of growth of the different sections, at least for the basal and central part of both cores, and to interpret this petrographic sequence in terms of the main changes in the climate system. A possible correlation among the different lithofacies and the SPECMAP curve (Martinson & *alii*, 1987) is reported in fig. 9 and discussed further below.

The darkest, lowermost section of the flowstone spans the period ca.160 to 130 ky and contains no major growth interruptions, suggesting very slow (mean growth rates ~1.07 mm/kyr) but continuous or near-continuous calcite precipitation during the last part of the penultimate glacial period, corresponding to the end of MIS6 (fig. 9). The observed lamination in the clastic content of the bottom part of core D3 (Section 1, fig. 4a) reinforces this interpretation, suggesting a situation of very low percolation rates, with the flowstone covered by a continuous film of percolation water rich in impurities, which were deposited in the space between the crystals without disturbing their slow growth. Alternatively, the thin clastic layers were deposited during phases of high discharge then the continuous crystal growth deformed the previous layers which remains embedded in the vacuum between crystals. The absence of this specific fabric for the same period of growth of the other cores (D4) may be explained in terms of lateral variability of the water film, related to the past shape of the flowstone and/or differences in the sources of drip waters (it is worth nothing that the flowstone is laterally extensive and is fed by waters entering from different fractures).

The boundary between the Lf-A and the white, detrital-poor calcite of Lf-B is broadly fixed around 130 ka, close to the MIS6-MIS5 transition (fig. 9). This drastic

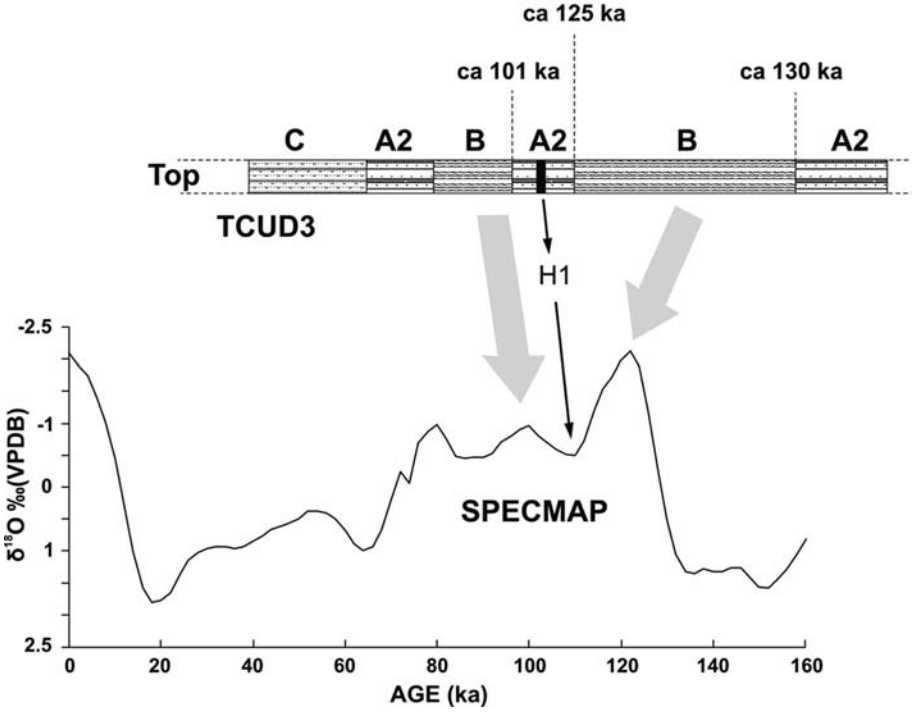

FIG. 9 - Proposed correlation between the SPECMAP curve (Martinson & *alii*, 1987) and the stratigraphy of TCU flowstone.

change in the global climatic conditions is known as Termination II in the marine record (Martinoson & *alii*, 1987; Pailler & Bard, 2002; Martrat & *alii*, 2004; Skinner & Shackleton, 2006) and is chronologically constrained at Corchia at ca.135 ka (Drysdale & *alii*, 2005; 2009).

Radiometric ages allow us to assign full interglacial conditions of MIS5e to the onset of Lf-B facies in both cores, corresponding to sections 3 and 9 (fig. 3). Here, we observe the highest growth rates (18 mm/kyr) and lower impurities, indicating high discharge within the cave, with enhanced calcite deposition and dilution or cessation of input of impurities. The high rainfall amount thought to be responsible for this high water flux is in good agreement with other records of the same periods: Corchia speleothems (Drysdale & *alii*, 2004; 2009) for the Apuan Alps but also the pluvial period recorded in Soreq and Peqiin cave in Israel (Bar-Matthews & *alii*, 2000; 2003) and in Bourgeois-Delaunay cave in South-west France (Couchoud & *alii*, 2009), suggesting that Eastern Mediterranean and western Europe experienced relatively wet conditions simultaneously during this part of the last interglacial.

The beginning of the first section of white calcite (sections 3 and 9) is quite well defined between 135 and 130 ka, in agreement with the chronology proposed by Drysdale & *alii*, 2005 for the same events in Corchia. On the contrary, the timing of the end of this sequence and many more of the following sections 4 and 10 belonging to Lf-A (which is crossed in both cores by the Hiatus H1) is difficult to constrain. The last age available before the end of the Lf-B is about 124.3 ± 1.35 ka, whereas the first date after the growth interruption H1 is already in the Lf-B, section 5 (white, inclusion-poor calcite) and indicates an age of 101.5 ± 3.3 ka. This time interval spans from the last part of MIS5e to the early part of the MIS5c (fig. 9), and allows us to link the second incidence of brown, inclusion-rich calcite of Lf-A (section 4 and 10) to the climatic deterioration after MIS5e. Studies from the high-latitude North Atlantic, in fact, show that the post-MIS 5e climate was very unstable (McManus & *alii*, 1994; Chapman & Shackleton, 1999), with at least two major cold events, known as C23 and C24, recorded in sub-polar North Atlantic marine cores, the influence of which was felt in the middle latitudes (Heusser & Oppo, 2003; Lehman & *alii*, 2002; Sanchez-Goñi & *alii*, 2005). These events have been correlated with the Mélisey I and Montaigu cold stages recognized in western European lake pollen records (Woillard, 1978; De Beaulieu and Reille, 1984). These cold events recognized in Europe are also in broad agreement with Greenland stadials GS25 (111.0-108.5 ka) and GS24 (106.0-104.5 ka) recorded in the NGRIP ice cores (North Greenland Ice Core Project Members [NGRIP], 2004), suggesting major disruption to North Atlantic circulation due to the southward shift of Polar Front (Sánchez Goñi & *alii*, 1999). An independent radiometric chronology for these events was provided by Drysdale & *alii* (2007), with the older event extending between ca. 112.0 ± 0.8 ka and 108.8 ± 1.0 ka, and the younger commenced at 105.1 ± 0.9 ka and ended at 102.6 ± 0.8 ka. The ages of these events broadly overlap the second section of Lf-A (section 4 and 10) and the H1 in TCU cores, although the warmer interval between the two major events is missing in the stratigraphy of the flowstone, perhaps due to erosion or dissolution associated with the formation of H1. This hiatus thus most likely demarcates the onset of stadial conditions

identified throughout the North Atlantic and which had a major impact on the climate of Europe (Shackleton & *alii*, 2002; Müller & Kukla, 2004; Meyer & *alii*, 2012).

The last age available for the sequence is in section 5 (white inclusion-poor calcite of Lf-B), and indicates an age of 101.52 ± 1.3 ka., corresponding to MIS5c in the marine stratigraphy (fig. 9). The re-commencement of the white calcite suggests a new period of high precipitation. For MIS5c many studies suggest a marked climatic amelioration following the C23 and C24 cold events. This is visible both in marine (McManus & *alii*, 1994; Sánchez Goñi & *alii*, 1999, 2005 Martrat & *alii*, 2004) and in continental records (North Greenland Ice Core Project Members, 2004; Drysdale & *alii*, 2007).

As stated earlier, the upper part of TCU flowstone lacks any chronological constraint so it is not possible to disentangle its palaeoenvironmental signal and discuss possible correlations with other archives. In any case, the presence of the third section of Lf-A (section 6) suggests another period of slow growth/low precipitation. The subsequent presence of the lithofacies C (different from all the previous section) and, subsequently, the terminal sections with its series of growth interruptions (maybe associated with erosion), suggest that at least some of the environmental parameters changed fundamentally (and persistently) for Tana che Urla Cave.

Finally, it is interesting to note that, while the penultimate glacial (i.e. MIS6) is represented in the bottom part of the TCU flowstone, the last glacial period seems to be largely missing or characterised by a series of hiatuses (not deposited or subsequently re-eroded). This lack of a continuous last glacial sequence could simply be a matter of change in the flowstone's feeding system, but the Holocene age at the top of the core suggests that there was no significant alteration of water flow source during the entire period of flowstone growth. If this premise is correct, it may suggests that MIS6 in the Apuan Alps was not as severe as the last glacial period (MIS4-2). In fact the deposition of the flowstone, even though very slow, was continuous during at least the last part of MIS6 whereas it stopped, probably for a long time, during the last glacial period. The idea of a «milder» continental MIS6 compared to Last Glacial is not new: some data from Argentarola cave, in southern Tuscany (Bard & *alii*, 2002) and from Soreq cave in Israel (Aylon & *alii*, 2000) highlight the presence of at least two humid events for this period, the older of which is thought to be related with the deposition of Sapropel S6. Moreover, Corchia Cave suggests continuous growth during most part of MIS6 (Drysdale & *alii*, 2005, 2009; Zanchetta & *alii*, 2005) but, so far, no continuous records are available for the Last Glacial from this cave.

CONCLUSIONS

The chronologically constrained part of the studied flowstone consists of an alternation of two different lithofacies: a brown, detrital-rich calcite (Lf-A) and a white, detrital-poor calcite (Lf-B), both with columnar fabric. The lower section of this succession, including both lithofacies, precipitated between ca 160 and 124 ka, while the upper part starts before 101 ka and ends with a series of growth interruptions that are not well defined chronologically. The two sections are separated by a hiatus between ca. 124 and 101 ka.

This study suggests that these petrographic changes are the result of climate fluctuations that impacted on the Apuan Alps area. The white-clastic poor calcite seems to be the result of higher growth rates, due to high infiltration related to wet (interstadial) conditions and clastic flux prevented by soil development in the cave's catchment, while the brown-clastic-rich calcite is thought to be due to a reduction of the precipitation during dry (stadial) phases, when soil erosion is enhanced in a climate colder and drier. The available U/Th ages allow us to correlate the first section of brown calcite (lithofacies A, Sections 1,2 and 8) with MIS6, and the first section of white calcite (Lf-B, sections 3 and 9) to full interglacial conditions of MIS5e. Moreover, it is possible to propose that the hiatus H1 correlates with the stadial period corresponding to MIS5d. For the upper part of the sequence, above H1, the chronology is not well defined but the last U/Th age available suggests that section 5 and 11 (lithofacies B, white, inclusion-poor calcite) may have formed during MIS 5c (fig. 9). This implies that Tana che Urla Cave is sensitive to the main shifts in the global climatic system.

The proposed interpretation confirms the general conclusions obtained from other records in the area (e.g. Corchia Cave) on which the passage from glacial to interglacial is dominated by a dramatic shift in the amount of meteoric precipitation. It is interesting to note that the transition from lithofacies A to lithofacies B is almost coincident (within errors and chronological problem of Tana che Urla) with the isotopic transition defined by Drysdale & *alii* (2005; 2009) at Corchia between MIS6-5.

Finally, we would highlights that, contrary to the upper part of the successions which is characterised by several *hiati*, suggesting conditions unfavourable for speleothems growth, during most of MIS6 (although with low growth rate) no significant *hiati* are observed. This suggests that the MIS6 glacial period was milder than MIS4-2 in the Apuan Alps (Zanchetta & *alii*, 2005).

REFERENCES

AYALON A., BAR-MATTHEWS M. & KAUFMAN A. (1999) -*Petrography, strontium, barium and uranium concentrations, and strontium and uranium isotope ratios in speleothems as palaeoclimatic proxies: Soreq Cave, Israel.* The Holocene 9, 715-722.

AYALON A., BAR-MATTHEWS M. & KAUFMAN A. (2002) - *Climatic conditions during marine isotope stage 6 in the eastern Mediterranean region from the isotopic composition of speleothems of Soreq Cave, Israel*. Geology, 30; 303-306.

BARD E., DELAYGUE G., ROSTEK F., ANTONIOLI F., SILENZI S. & SCHRAG D.P. (2002) - *Hydrological conditions over the western Mediterranean basin durino the depositino of the cold Sapropel 6 (ca. 175 kyrBP).* Earth and Planetary Science Letters, 202, 481-494.

BARD E., ANTONIOLI F. & SILENZI S. (2002) - *Sea-level during the penultimate glacial period based on a submerged stalagmite from Argentarola cave (Italy).* Earth and Planetary Science Letters, 196, 135-146.

BAR-MATTHEWS M., M.A. AYALON A., GILMOUR M., MATTHEWS A. & HAWKESWORTH C.J. (2003) - *Sea-land oxygen isotopic relationships from planktonic foraminifera and speleothems in the eastern Mediterranean region and their implication for paleorainfall during interglacial intervals*. Geochimica e Cosmochimica Acta, 67, 3189-3199.

BAR-MATTHEWS M., M.A. AYALON A. & KAUFMAN A. (2000) -*Timing and hydrological conditions of sapropel events in the Eastern Mediterranean, as evident from speleothems, Soreq Cave, Israel.* Chemical Geology, 169, 145-156.

BOLLE H.J. (2003) - *Climate, climate variability, and impacts in the Mediterranean area: an overview*. In: H.-J. Bolle (Ed.), «Mediterranean Climate: Variability and Trends», Springer, Berlin, 5-86.

CARMIGNANI L. & KLINGFIELD R. (1990) - *Crustal extension in the Northern Apennines: the transition from compression to extension in the Alpi Apuane Core Complex*. Tectonics, 9, 1275-1303.

CARMIGNANI L., CONTI P., DISPERATI L., FANTOZZI P.L., GIGLIA G. & MECCHERI M. (2000) - *Carta geologica del Parco delle Alpi Apuane, scala 1:50000*. Selca, Firenze.

CHACO I., J.O. GRIMALT C., PELEJERO M. CANALS F.J. SIERRO J.A. & FLORES N. (1999) - *Shackleton, Dansgaard-Oeschger and Heinrich event imprints in Alborean Sea paleotemperatures*. Paleoceanography, 14, 698-705.

CHAPMAN M.R. & SHACKLETON N.J. (1999) - *Global ice-volume fluctuations, North Atlantic ice-rafted events, and deep-ocean circulation changes between 130 and 70 ka*. Geology, 27, 795-798.

COUCHOUD I., GENTY D., HOFFMANN D., DRYSDALE R.N. & BLAMART D. (2009) -*Millennial-scale climate variability during the Last Interglacial recorded in a speleothem from south-western France*. Quaternary Science Reviews, 28, 3263-3274.

DE BEAULIEU J.L. & REILLE M. (1984) - *A long upper Pleistoncene pollen record from Les Echets, near Lyon, France.* Boreas, 13, 111-132.

DREYBRODT W. (1988) - *Processes in karst systems: physics, chemistry, and geology*. Springer-Verlag,12, 288, Berlin, New York.

DRYSDALE R.N., ZANCHETTA G., HELLSTROM J.C., FALLICK A.E., ZHAO J.X., ISOLA I., & BRUSCHI G. (2004) - *Palaeoclimatic implications of the growth history and stable isotope ($\delta^{18}O$ and $\delta^{13}C$) geochemistry of a Middle to Late Pleistocene stalagmite from central-western Italy*. Earth and Planetary Science Letters, 227, 215-229.

DRYSDALE R.N., ZANCHETTA G., HELLSTROM J.C., FALLICK A.E. & ZHAO J.X. (2005) - *Stalagmite evidence for the onset of the Last Interglacial in southern Europe at 129±1 ka.* Geophysical Research Letters, 32.

DRYSDALE R.N., ZANCHETTA G., HELLSTROM J.C., FALLICK A.E., MCCONALD J. & CARTWRIGHT I. (2007) - *Stalagmite evidence for the precise timing of North Atlantic cold events during the early last glacial*. Geology, 35 (1), 77-80.

DRYSDALE R.N., ZANCHETTA G., HELLSTROM J.C., FALLICK A.E., SANCHEZ GONI M.F., COUCHOUD I., MC DONALD J., MAAS R., LOHMANN G. & ISOLA I. (2009) - *Evidence for obliquity forcing of glacial termination II*. Science, Vol. 325, 5947, 1527-1531.

FAIRCHILD I.J. & TREBLE P.C. (2009) - *Trace elements in speleothems as recorders of environmental change.* Quaternary Science Reviews, 28, 449-468.

FORD D.C. & WILLIAMS P.W. (1989) - *Karst Geomorphology and Hydrology*. Allen and Unwin, London.

FRISIA S., BORSATO A., FAIRCHIL I. & MCDERMOTT F. (2000) - *Calcite fabrics, growth mechanisms, and environments of formation in speleothems from the Italian Alps and southwestern Ireland*. Journal of Sedimentary Petrology, 70, 1183-1196.

FRISIA S., BORSATO A., PRETO N. & MCDERMOTT F. (2003) - *Late Holocene annual growth in three Alpine stalagmites records the influence of solar activity and the North Atlantic Ocillation on winter climate*. Earth and Planetary Science Letters, 216, 411-424.

FRISIA S. (2003) - *Le tessiture negli speleotemi.* Studi Trentini di Scienze Naturali, Acta Geologica, 80, 85-94.

GASCOYNE M. (1992) - *Palaeoclimate determination from cave calcite deposits*. Quaternary Science Reviews, 11, 609-632.

GENTY D., BLAMART D., OUAHDI R., GLIMOUR M., BAKER A., JOUZEL J. & VAN-EXTER S. (2003) - *Precise dating of Dansgaard-Oeschger climate oscillations in western Europe from stalagmite data.* Nature, 421, 833-837.

GONZALEZ L.A., CARPENTER S.J. & LOHMANN K.C. (1992) - *Inorganic calcite morphology: roles of fluid chemistry and fluid flow*. Journal of Sedimentary Petrology, 62, 382-399.

HELLSTROM J.C. (2006) - *U-Th dating of speleothems with high initial 230Th using stratigraphical constraint.* Quaternary Geochronology, 1, 289-295.

HELLSTROM J.C. (2003) - *Rapid and accurate U/Th dating using parallel ion-counting multi-collector ICP-MS*. Journal of Analytical Atomic Spectrometry, v. 18, 1346-1351.

HEUSSER L. & OPPO D. (2003) - *Millennial- and orbital-scale climate variability in southeastern United States and in the subtropical Atlantic during Marine Isotope Stage 5: evidence from pollen and isotopes in ODP Site 1059*. Earth and Planetary Science Letters, 214, 3-4, 483-490.

LAURITZEN S.-E. & LUNDBERG J. (1999) - *Speleothems and climate*. Holocene, 9, 643-647.

LEHMAN S.J., SACHS J.P., CROTWELL A.M., KEIGWIN L.D. & BOYLE E.A. (2002) - *Relation of subtropical Atlantic temperature, high-latitude ice rafting, deep water formation, and European climate 130,000-60,000 years ago.* Quaternary Science Review, 21, 18-19, 1917-1924.

LI W., LUNDBERG J., DICKIN A.P., FORD D.C., SCHWARTZ H.P., MAC NUTT R. & DORALE J.A. (1989) - *High precision mass spectrometric uranium series dating of cave deposits and implications for palaeoclimatic studies.* Nature, 339, 534-536.

JAILLET S., PONS-BRANCHU E., MAIRE R., HAMELIN B. & BRULHET J. (2006) - *Record of holocene palaeo-groundwater floods in two stalagmites of the Rupt-Du-Puits Sytem (Barrois, France). Morphological analysis of laminae and U/Th tims datings*. Geologica Belgica, 9, 297-307.

MARTINSON D.G., PISIAS N.G., HAYS J.D., IMBRIE J., MOORE T.C. & SHACKLETON N.J. (1987) - *Age dating and the orbital theory of the ice ages: development of a high resolution 0 to 300,000-year chronostratigraphy*. Quaternary Research, 27, 1-29.

MARTRAT B., GRIMAULT J.O., LOPEZ-MARTINEZ C., CACHO I., SIERRO F.J., FLORES J.A., ZAHAN R., CANALS M., JASON H.C. & HODELL D.A. (2004) - *Abrupt temperature changes in the Western Mediterranean over the past 250,000 years*. Science, 306 (5702), 1762-1765.

MCMANUS J.F., BOND G.C., BROECKER W.S., JOHNSEN S., LABEYRIE L. & HIGGINS S. (1994) - *High resolution climate records from the North Atlantic during the last interglacial.* Nature, 371, 326-329.

MEYER M.C., SPOTL C., MANGINI A. & TESSADRI R. (2012) - *Speleothems deposition at the glaciation threshold: An attempt to constrain the age and paleoenvironmental significance of a detrital-rich flowstone sequence from Entrische Kirche Cave (Austria).* Palaeogeography, Palaeoclimatology, Palaeoecology, 93, 106, 319-320.

MULLER U.C. & KUKLA G.J. (2004) - *North Atlantic Current and European environments during the declining stage of the Last Interglacial*. Geology, 32,1009-1012.

NIGGEMANN S., MANGINI A., RICHTER D.K. & WURTH G. (2003) - *A paleoclimate record of the last 17 600 yr in stalagmites from the B7 cave, Saurland, Germany*. Quaternary Science Reviews, 22, 555-567.

NORTH GREENLAND ICE CORE PROJECT (2004) - *High resolution record of Northern Hemisphere climate extending into the last interglacial period.* Nature, 431, 147-151.

PAILLER D. & BARD E. (2002) - *High frequency palaeoceanographic changes during the past 140.000 yr recorded by the organic matter in sediments of the Iberian Margin*. Palaeogeography, Palaeoclimatology, Palaeoecology, 181, 4, 431-452.

PICCINI L. (1997) - *Evolution of karst in the Alpi Apuane (Italy): relationships with the morphotectonic history*. Supplementi, Geografia Fisica e Dinamica Quaternaria, 4, 21-31.

PICCINI L. (2011) - *Speleogenesis in highly geodynamic contexts: The quaternary evolution of Monte Corchia multi-level karst system (Alpi Apuane, Italy)*. Geomorphology, 134, 1-2, 49-61.

PICCINI L., PRANZINI G., TEDICI L. & FORTI P. (1999) - *Le risorse idriche dei complessi carbonatici del comprensorio apuo-versiliese*. Quaderni Geologia Applicata, 6-1, 61-78.

PICCINI L., BORSATO A., FRISIA S., PALADINI M., SALZANI R., SAURO U. & TUCCIMEI P. (2003) - *Concrezionamento olocenico e aspetti geomorfologici della Grotta del Vento (Alpi Apuane - Lucca): analisi paleoclimatica e implicazioni morfogenetiche.* Studi Trentini di Scienze Naturali, Acta Geologica, 80, 127-138.

PICCINI L., DRYSDALE R.N. & HEIJNIS H. (2003) - *Karst caves morphology and sediments as indicators of the uplift history in the Alpi Apuane (Tuscany, Italy).* Quaternary International, 101-102, 219-227.

PICCINI L., ZANCHETTA G., DRYSDALE R.N., HELLSTROM J.C., ISOLA I., FALLICK A.E., LEONE G., DOVERI M., MUSSI M., MANTELLI F., MOLLI G., LOTTI L., RONCIONI A., REGATTIERI E., MECCHERI M. & VASELLI L. (2008) - *The environmental features of the Monte Corchia cave system (Apuan Alps,central Italy) and their effects on speleothem growth.* International Journal of Speleology, 37, 3, 153-172.

SANCHEZ GONI M.F., EYNAUD J., TURON L. & SHACKLETON N.J. (1999) - *High resolution palynological record off the Iberian margin: direct land-sea correlation for the Last Interglacial complex*. Earth and Planetary Science Letters, 171, 1, 15, 123-137.

SANCHEZ GONI M.F., LOUTRE M.F., CRUCIFIX M., PEYRON O., SANTOS L., DUPRAT J., MALAIZE B., TURON J.L. & PEYPOUQUET J.P. (2005) - *Increasing vegetation and climate gradient in Western Europe over the Last Glacial Inception (122-110 ka): datamodel comparison*. Earth and Planetary Science Letters, 231, 111-130.

SHACKLETON N.J., CHAPMAN M., SANCHEZ GONI M.F., PAILLER D. & LANCELOT Y., (2002) - *The classic marine isotope substage 5e*. Quaternary Research, 58, 14-16.

SKINNER L.C. & SHACKLETON N.J. (2006) - *Deconstructing Terminations I and II: revisiting the glacioeustatic paradigm based on deep-water temperature estimates.* Quaternary Science Reviews, 25, 23-24, 3312-3321.

SPOTL C. & MANGINI A. (2002) - *Stalagmite from the Austrian Alps reveals Dansgaard-Oschger events during isotope stage 3: implications for the absolute chronology of Greenland ice cores*. Earth Planetary Science Letters, 203, 507-518.

SPOTL C., MANGINI A., FRANK N., EICHSTADTER R. & BURNS S. (2002) - *Start of the last interglacial period at 135 ka: evidence from a high Alpine speleothems.* Geology, 30, 815-818.

TRIGO I.F., BIGG G.R. & DAVIES T.D., (2002) - *Climatology of cyclogenesis mechanisms in the Mediterranean.* Monthly Weather Review, 130, 549-569.

VALLISNERI A. (1723) - *Lezione accademica sull'origine delle Fontane.*

WANG Y.J., CHENG H., EDWARDS R.L., AN Z.S., WU J.Y., SHEN C.C. & DORALE J.A. (2001) - A *high resolution absolute-dated Late Pleistocene monsoon record from Hulu cave, China.* Science, 294, 2345-2348.

WOILLARD G. (1978) - *Grande Pile peat Bog: a continuous pollen record for the last 140.000 years.* Quaternary Research, 9, 1-21.

ZANCHETTA G., DRYSDALE R.N., HELLSTROM J.C., FALLICK A.E., ISOLA I., GAGAN M. & PARESCHI M.T. (2007) - *Enhanced rainfall in the western Mediterranean during deposition of sapropel S1: stalagmite evidence from Corchia cave (Central Italy)*. Quaternary Science Reviews, 26, 279-286.

ZANCHETTA G., DRYSDALE R.N., HELLSTROM J.C., FALLICK A.E., ISOLA I., BRUSCHI G. & RONCIONI A. (2005) - *L'archivio climatico preservato all'interno delle stalagmiti dell'Antro del Corchia (Alpi Apuane, Italia centrale).* Atti del convegno: Le grotte raccontano, Memorie dell'Istituto Italiano di Speleologia, 2, 18, 161-176.

ZHORNYAK L.V., ZANCHETTA G., DRYSDALE R.N., HELLSTROM J.C., ISOLA I., REGATTIERI E., PICCINI L., BANESCHI I. & COUCHOUD I. (2011) - *Stratigraphic evidence for a «pluvial phase» between ca 8200-7100 ka from Renella cave (Central Italy)*. Quaternary Science Reviews, 30, 409-417.

(Ms. received 30 July 2012; accepted 31 October 2012)